The hydrogeology of the deep groundwater system in the Hammamet–Nabeul regional basin, north-eastern Tunisia: a hydrochemical and isotopic approach

Amor Ben Moussa, Kamel Zouari & Fayçal Jlassi

Carbonates and Evaporites

ISSN 0891-2556
Volume 26
Number 4

Carbonates Evaporites (2011)
26:327-338
DOI 10.1007/s13146-011-0069-y

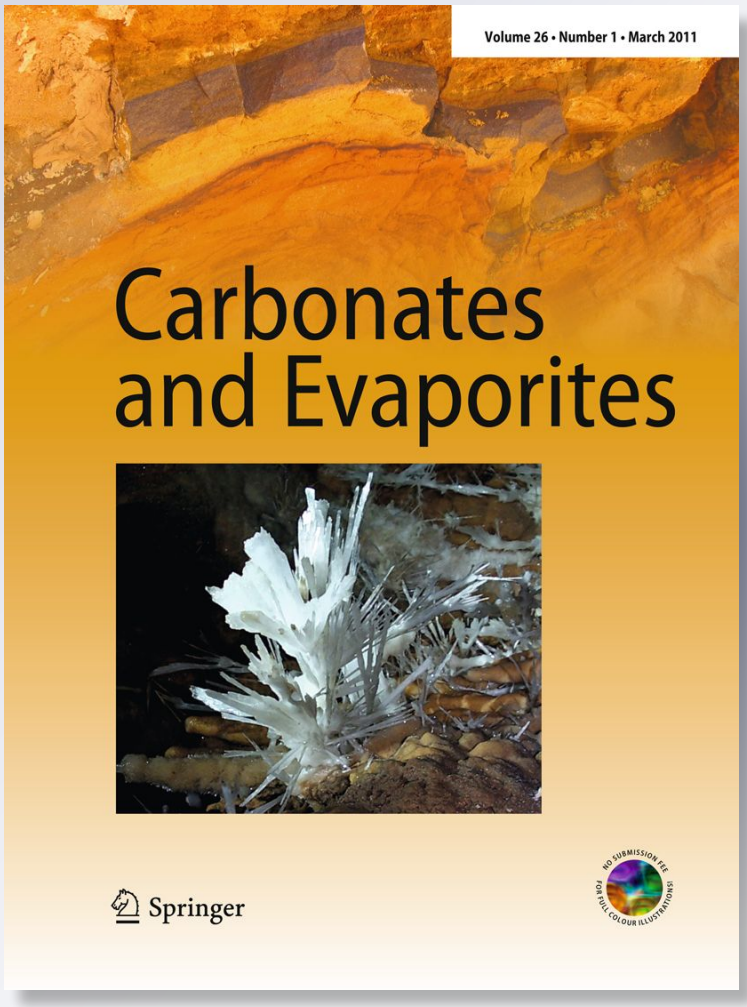

Springer

Carbonates Evaporites (2011) 26:327–338
DOI 10.1007/s13146-011-0069-y

ORIGINAL ARTICLE

The hydrogeology of the deep groundwater system in the Hammamet–Nabeul regional basin, north-eastern Tunisia: a hydrochemical and isotopic approach

Amor Ben Moussa · Kamel Zouari · Fayçal Jlassi

Accepted: 9 September 2011 / Published online: 14 October 2011

Abstract The scarcity of surface water in the Hammamet–Nabeul regional basin has imposed an over-abstraction of groundwater resources to meet the population demand for touristic and agricultural sectors. The impact of such a groundwater management on the aquifer system hydrodynamics and water quality has been investigated using a set of hydrochemical and isotopic data. Furthermore, a better understanding of the mineralization processes, the groundwater origins and the sources of recharge have been provided. Four water types were recognized; Na–HCO_3, Ca–HCO_3, Ca–SO_4–Cl and Na–Cl. They are in relation with water–rock interaction processes i.e. the dissolution of evaporates and the cation exchange. Stable isotopes of water molecule (^{18}O and δ^2H) permit to identify three different groups. The first is characterized by relatively enriched isotope contents lending support to the important infiltration of recent rainwater in the foot of mountains. The second is distinguished by relatively depleted contents of stable isotopes reflecting a paleoclimatic origin. The third is marked by a significant enrichment of deuterium, which suggests a significant exchange with H_2S in relation with the bacterial reduction of sulfate.

A. Ben Moussa (✉) · K. Zouari
Ecole Nationale d'Ingénieurs de Sfax, B. P. "W",
3038 Sfax, Tunisia
e-mail: amor_geologie@yahoo.fr

F. Jlassi
Commissariat Régionale de Développement
Agricole de Nabeul, Nabeul, Tunisia

Keywords Hammamet–Nabeul basin · Deep groundwater system · Water–rock interaction · Recent recharge · Paleoclimatic origin · H_2S exchange

Introduction

The Hammamet–Nabeul basin is one of the semi-arid regions in the north-eastern Tunisia, which is characterized by low and irregular rainfall, high temperature and evapotranspiration. This basin faces immense pressures to deliver and manage groundwater resources. Problems are exacerbated by lack of precipitation, population growth and rapid economic growth. Groundwater from the Hammamet–Nabeul multilayer aquifer system continues to serve as a reliable source of water for variety of purposes, including industrial and domestic uses and irrigation. At present, more than 3,000 boreholes, with a depth ranging from 60 to more than 150 m, tap the different aquifer levels with a mean exploitation of 60 Mm^3/year (DGRE 2006). The expansion of the fresh-water demand has raised concerns relating to the effects of numerous new wells on this valuable groundwater resource as the rate of replenishment of the aquifers is not known. Hence, substantial overexploitation of groundwater has resulted in a transient state whose main short-term consequences were the generalized water-level decline and the decrease of discharge rates. Associated with these deleterious consequences, severely increasing overtime, some water quality degradation was registered in several zones of the basin.

The main objective of this study is to integrate hydrogeological data with major ions geochemistry and isotopic signatures of groundwater to clarify the hydrodynamic functioning of the aquifer system and identify the major hydrochemical processes that control the groundwater

mineralization. It also aims to provide information about the origin and migration pathways of water bodies.

Study area

The Hammamet–Nabeul basin, which belongs to the Cap Bon peninsula at the north-eastern part of Tunisia, is located in the western coast of the Sicilian Strait (Elmejdoub and Jedoui 2009). It covers a total area of about 450 km^2 and it is limited in the north by the Grombalia basin, in the east by the oriental coastal plain, the south by the Gulf of Hammamet, and in the west by the Bouficha basin (Fig. 1). This basin is characterized by a semi-arid, "Mediterranean" climate with mean annual values of precipitation, temperature, and potential evapotranspiration of about 450 mm, 20°C and 1,350 mm, respectively. Ground elevation in this basin varies from about 0 to 500 m AMSL. The drainage network is relatively dense and is constituted of several ephemeral wadis, which collect and transport surface runoff from the northern surrounding highlands toward the golf of Hammamet discharge area.

Geologically, the sedimentary formations out cropping in the Hammamet–Nabeul basin range from the Early Eocene to the Quaternary (Fig. 2). In the depth, the Eocene series, which represent the oldest deposits, are constituted by thick Ypresian limestone units of the Bou Dabbous Formation overlaid by the Lutetian–Priabonian marl of the Souar Formation (Ben Salem 1995; Mzali 2010). On the Eocene units reposes unconformably the Oligocene coarse to medium grained sandstone of the Fortuna Formation (Burollet 1956; Blondel 1991). This latter is covered by the Burdigalian clayey sand and sandstone of the Massiouta Formation, which is overlain by the Langhian limestone and gypseous marl of the Ain Ghrab and Mahmoud Formations, respectively. Above, lay the fine to medium grained sand deposits of the Beglia Serravalian Formation and the clay and marly clay series of the Souaf Tortonian Formation. On the Souaf deposits, repose the sandy units of the Somâa and Beni Khiar Tortonian Formations, which are overlain by the sandy sandstone of the Oued el Bir Messinean Formation. The Plio-Quaternary Formations, which overlay the Miocene series, are represented by the Lower Tabianian clay of Potters, the Upper Tabianian sands of Nabeul, the Lower Plaisancian clay of Sidi Barka, the Upper Plaisancian sandstones of Hammamet and the Quaternary sands of the Rejich Formation (Schoeller 1939; Colleuil 1976; Ben Salem 1995).

Hydrogeological setting

Hydrogeologically, the Hammamet–Nabeul basin contains an important multilayer aquifer system, which is constituted

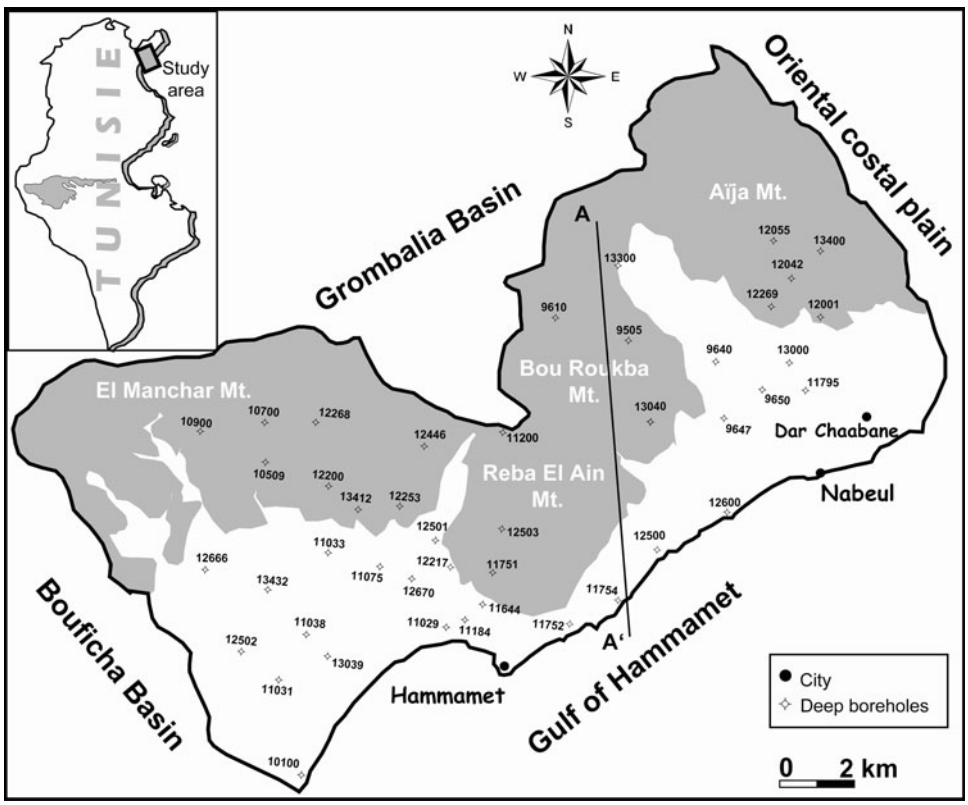

Fig. 1 Location and sampling map

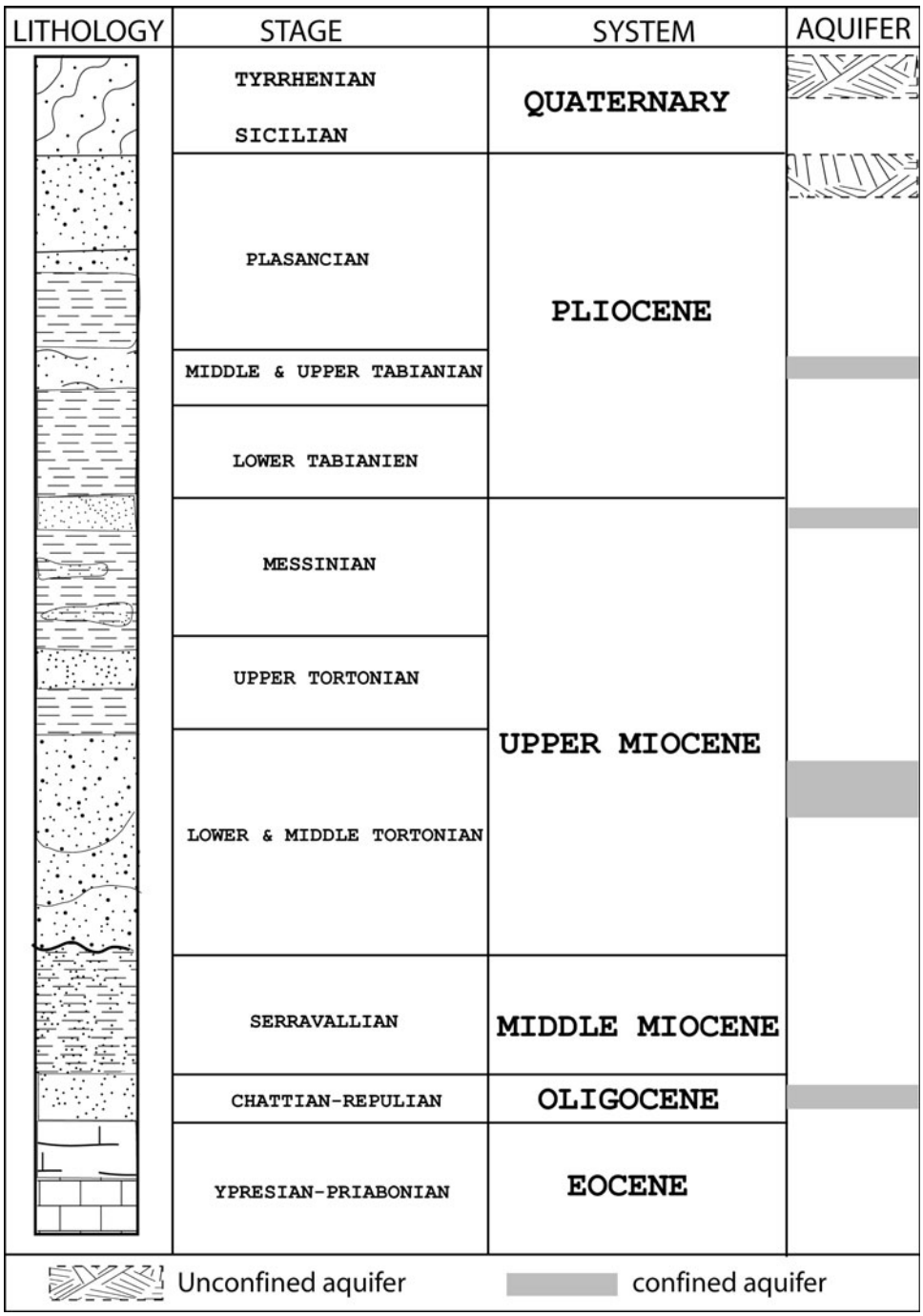

Fig. 2 Simplified litostratigraphic column of the Hammamet–Nabeul basin

by three superposed levels that locally communicate via faults and semi-permeable sedimentary units (Fig. 3). The Plio-Quaternary aquifer (PQ), which represents the shallowest level, exists only in the western part of the basin with an average thickness of about 150 m. It is unconfined only in the foot of the Reba el Ain Mountain. This confined/unconfined aquifer, which is taped by numerous shallow dug wells and deep boreholes, consists mainly of varying proportions of sandstone, sand, silt, clay and evaporate that repose on the Upper Miocene clayey deposit impermeable bedrock.

The Pliocene aquifer that corresponds to the intermediate level exists only in the eastern part of the basin and varies in thickness between 30 and 200 m. This confined aquifer, which is made up of sandstone, sands and clayey sands (Mzali et al. 2007), is tapped by several private deep boreholes with depths ranging from ca. 80 to 200 m.

The Middle Miocene deep aquifer is constituted of sands and clayey sands locally intercalated with thin discontinuous clay layers, which permit the hydraulic connectivity between the different aquifer levels. This aquifer is confined in major

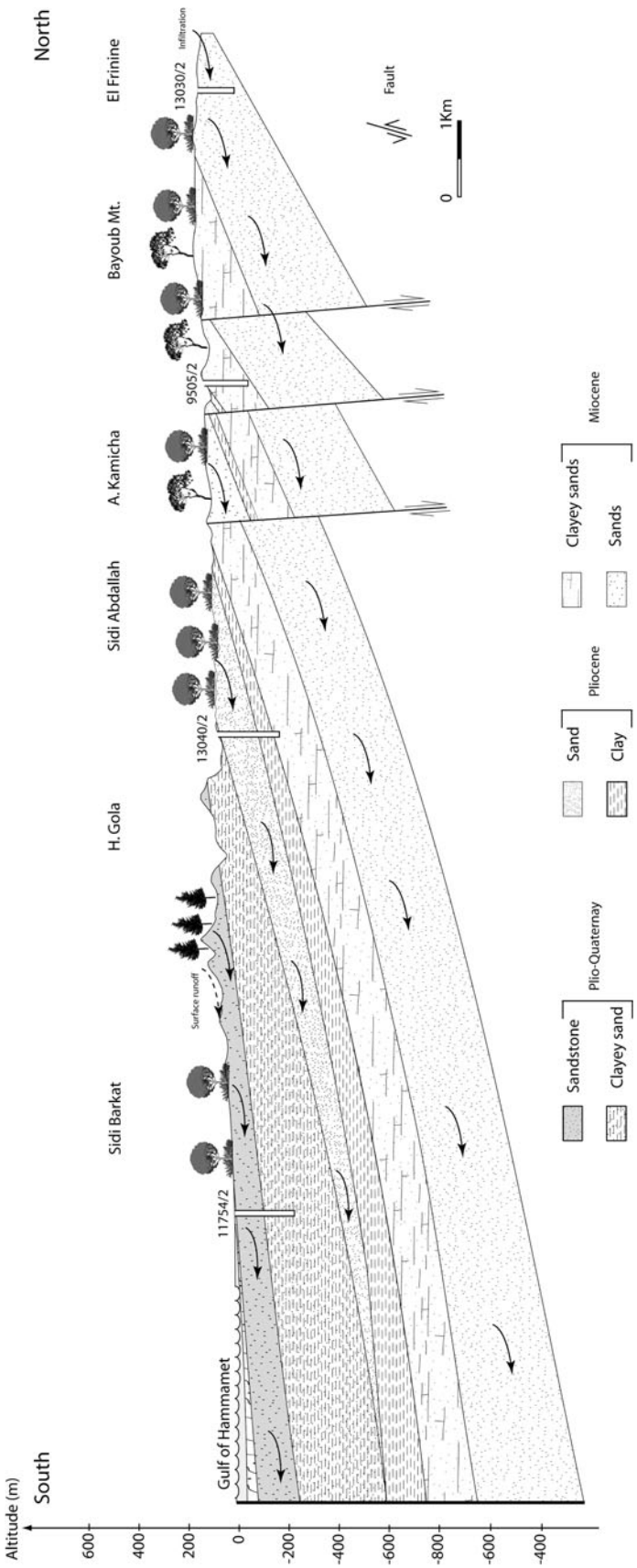

Fig. 3 Hydrogeological cross section in the Hammamet–Nabeul deep aquifer system

part of the basin, except in the eastern part where the overlying Pliocene aquifer was completely eroded. It is tapped by several private deep boreholes with depths ranging from ca. 60 to 150 m. This deep aquifer is separated from the overlying Pliocene aquifer by impermeable Upper Miocene units consisting of clayey and marl deposits.

Groundwater flow pattern in the Hammamet–Nabeul multilayer aquifer system is somewhat simple. Groundwaters converge N–S and NW–SE from the foot of El Manchar, Reba el Ain, Bou Rokba and Aïja Mountains, in the north of the basin, toward the gulf of Hammamet that represents the discharge zone. This may indicate that recharge rainwater infiltrates in the foot of the surrounding Mountains and converges to the Mediterranean Sea.

Analytical procedure

The sampling campaign was undertaken in the study area during March 2008. A total of 45 boreholes were sampled for geochemical and isotopic analyses. Temperature, pH and electrical conductivity were directly measured in the field using portable meters allowing temperature compensation and calibration with appropriate standards. TDS was determined by evaporating the sample and drying it at 105°C. Chemical analysis of the water samples were carried out in the "Laboratoire de Radio-Analyses et Environnement" of the School of Engineers of Sfax, Tunisia. Major cation concentrations were performed on a Waters Ion chromatograph using IC-Pak^{TM} CM/D columns. Major anion concentrations were measured using a Metrohm ion chromatograph equipped with CI SUPER-SEP columns. The analysis of bicarbonate was undertaken by titration to the methyl orange endpoint. Oxygen-18 and deuterium analyses were performed in the laboratory of the international agency of atomic energy (IAEA) in Vienna by employing, respectively, the standard CO_2 equilibration (Epstein and Meyada 1953) and the zinc reduction techniques (Coleman et al. 1982), followed by the analysis on a mass spectrometer. The results were reported to δ notation relative to Vienna standard mean oceanic water (VSMOW), where $\delta = [(R_S/\text{RSMOW}) - 1] \times 1{,}000$, R_S represents either the $^{18}O/^{16}O$ or the $^{2}H/^{1}H$ ratio of the sample, and RSMOW is $^{18}O/^{16}O$ or the $^{2}H/^{1}H$ ratio of the SMOW. Typical precisions are ± 0.1 and $\pm 1.0‰$ for oxygen-18 and deuterium, respectively.

Results and discussion

Hydrochemical composition of groundwater

In situ measurements and the overall geochemical characteristics of the Hammamet–Nabeul groundwater are presented in Table 1. The groundwater temperatures are relatively heterogeneous; they vary between 19° and 29.3°C, reflecting the interference of several factors, i.e. the screened depth intervals, the groundwater residence time from the recharge area and the rate of mixing. The EC values vary in a wide range from 0.7 to 5.5 μScm^{-1}. This significant variation is likely in relation with the variation of the TDS values, which oscillate largely between 0.146 and 3.27 mg L^{-1}.

Groundwater samples are plotted on the Piper diagram to precisely illustrate the difference between groundwater facies and their geochemical change (Piper 1944). According to this diagram, groundwater samples were classified into four major water types that correspond to Na–HCO_3, Ca–HCO_3, Ca–SO_4–Cl and Na–Cl (Fig. 4).

Correlations between major ions are useful because they permit to identify associations involving elements that can show the same origin. It can also point out the participation of major mineralization processes, which commonly occurs in hydrochemistry. The well-defined relationships, which typify the plots of the $\sum$ anions versus Cl and SO_4, as well as the $\sum$ cations versus Na, Ca and Mg provide insight into the contribution of the aforementioned ions to the groundwater mineralization (Fig. 5). The plot of Na versus Cl exhibits a well-defined relationship, indicating that the dissolution of halite may exert a control on the Na^+ and Cl^- concentrations (Fig. 6). The dissolution of NaCl is, however, verified through the negative saturation indices that indicate an undersaturation state of groundwater with respect to halite. The plot of Ca versus SO_4 shows that groundwater samples collected from the unconfined aquifer define a linear trend, reflecting the contribution of gypsum and/or anhydrite to the chemical composition of these groundwater samples (Fig. 7). However, the majority of samples collected from the confined aquifer fall above the line 1:1 indicating an obvious deficiency of SO_4 probably in relation with the sulfate reduction process. The organic reduction of sulfate that is catalyzed by bacteria represents a significant microbial process, which characterizes such a confined environment (Jorgensen 1982; Compton 1988; Lyons et al. 1984; Last 1990). The net reaction for the bacterial sulfate reduction process is (Gomis-Yagues et al. 2000):

$$SO_4^{2-} + 2CH_2O\ (MO) \rightarrow H_2S + 2HCO_3$$

On the other hand, the inverse proportional evolution in the plot of $((Ca + Mg) - (HCO_3) + (SO_4))$ versus (Na + K–Cl) provides insight into the significant role played by the cation-exchange process in the groundwater mineralization of the Hammamet–Nabeul groundwater (Fig. 8).

Table 1 In situ measurements, geochemical and isotopic data of Hammamet–Nabeul deep aquifer groundwater

Aquifer	Boreholes (N IRH)	T (°C)	pH	TDS (mg/l)	Cl (meq/l)	SO_4 (meq/l)	HCO_3 (meq/l)	NO_3 (meq/l)	Na (meq/l)	Mg (meq/l)	Ca (meq/l)	Saturation indices					% o versus SMOW	
												Anhydrite	Calcite	Dolomite	Gypse	Halite	^{18}O	^{2}H
Unconfined aquifer	12670	22.7	7.9	1,020	1.2	9.6	5.3	0.0	9.5	3.0	3.0	−1.44	0.44	1.10	−1.20	−6.65	−5.23	−31.04
	12217	20.6	7.7	660	2.2	2.7	4.3	0.1	2.8	2.5	4.2	−1.73	0.43	0.73	−1.47	−6.90	−5.05	−28.61
	12501	22.5	7.8	700	2.2	2.5	4.7	0.0	3.2	2.7	2.8	−1.91	0.42	0.95	−1.67	−6.83	−5.2	−28.93
	13039	22.6	7.2	3,170	22.5	17.9	5.0	0.5	25.8	11.3	13.0	−0.83	0.29	0.66	−0.59	−5.00	−5.32	−32.33
	11184	19.3	7.8	870	21.0	7.1	5.3	0.0	17.2	9.8	9.8	−1.97	0.35	0.87	−1.68	−6.08	−5.26	−29.24
	11029	21.6	7.7	780	5.1	3.0	5.4	0.0	7.9	3.1	2.5	−1.95	0.54	0.85	−1.69	−6.26	−5.25	−30.28
	12446	22	7.6	1,720	8.2	5.2	6.8	0.0	11.4	4.8	4.2	−1.56	0.50	0.90	−1.31	−5.89	−5.28	−31.98
	12666	23.2	7	1,090	3.5	9.2	1.0	0.0	5.0	4.4	7.4	−0.13	0.37	0.77	0.11	−4.54	−5.31	−32.16
	11038	19	7.5	2,800	4.2	2.9	4.8	0.0	6.4	2.9	2.5	−1.21	0.53	1.21	−0.93	−5.09	−5.21	−28.33
	11075	22.6	7.4	2,450	27.8	9.3	5.9	0.0	39.4	4.0	3.7	−1.43	0.32	0.85	−1.20	−5.64	−5.04	−28.22
	10900	22.2	7		10.5	6.3	5.6	0.0	11.5	6.0	7.0	−1.91	0.65	1.32	−1.65	−6.54	−5.1	−32.37
	12253	21.7	7.3	1,830	20.1	8.1	5.2	0.0	24.7	5.2	4.7	−2.04	0.41	0.93	−1.79	−6.70	−5.22	−28.95
Confined aquifer	13040	20.5	8.2	550	22.5	17.9	5.0	0.5	25.8	11.3	13.0	−2.17	0.80	1.61	−1.90	−6.63	−5.73	−32.69
	13432	24.7	7.7	880	19.8	10.9	6.6	0.0	22.8	9.0	7.7	−2.21	0.10	0.50	−1.99	−5.97	−5.98	−35.38
	12502	22	7.8	3,270	5.5	2.7	4.9	0.0	9.5	1.9	1.3	−1.54	0.51	1.18	−1.30	−4.71	−6.08	−34.13
	11031	22.7	7.7	2,580	7.7	10.4	7.0	0.0	15.7	3.7	3.2	−1.45	0.51	1.20	−1.21	−5.04	−5.59	−33.98
	13412	22.4	7.5	1,430	10.3	1.6	5.4	0.3	5.5	6.0	6.3	−1.58	0.36	0.90	−1.33	−5.74	−5.65	−32.32
	12268	22	7.5	1,090	10.3	3.1	4.0	0.0	6.3	4.6	7.2	−1.74	0.30	0.65	−1.49	−6.13	−5.8	−35.07
	11033	24	7.6	1,710	16.1	8.0	6.2	0.0	11.1	8.8	37.9	–	–	–	–	–	−5.62	−33.04
	10509	24	7.8	820	5.6	2.9	5.0	0.0	6.5	3.8	4.4	−2.07	0.36	0.96	−1.84	−6.09	−5.87	−36.35
	10700	22.6	7.4	1,720	5.3	2.3	5.2	0.0	7.6	2.8	2.2	−1.33	0.38	0.81	−1.09	−5.64	−5.57	−33.36
	11644	21.3	7.9	710	3.5	2.1	3.2	0.0	3.9	3.1	3.7	−1.54	0.56	1.34	−1.29	−5.68	−5.47	−31.62
	12503	22.2	7.7	610	2.6	1.8	4.2	0.0	3.6	3.0	2.9	−1.90	0.28	0.63	−1.65	−5.95	−5.64	−32.36
	12500	22.1	7.7	146	6.9	5.3	6.1	1.2	15.9	6.2	4.9	−1.54	0.56	1.34	−1.29	−5.68	−5.48	−30.25
	11754	20.3	7.8	900	2.3	1.6	4.2	0.0	4.7	2.1	2.4	−2.27	0.30	0.84	−2.00	−6.20	−5.58	−31.69
	11751	22.3	7.8	770	3.2	2.2	5.8	0.0	9.5	2.1	1.5	−1.87	0.43	0.90	−1.62	−6.92	−5.57	−28.16
	11752	22.4	7.5	2,750	2.3	2.2	3.8	0.7	2.5	2.9	3.5	−1.24	0.55	1.21	−1.00	−5.19	−5.33	−28.77
	9647	29.3	8.2	650	7.0	1.0	6.6	0.1	5.7	6.2	5.0	−2.71	0.31	0.94	−2.54	−6.33	−5.91	−27.47
	9650	25.1	7.8	680	2.9	1.7	4.8	0.1	7.9	0.7	0.5	−2.12	0.60	1.42	−1.91	−6.39	−5.99	−27.51
	9640	21.6	8.2	620	3.3	1.7	5.2	0.0	6.0	3.1	2.6	−2.36	0.82	1.70	−2.11	−6.62	−6.01	−28.76
	13030	21.8	7.4	630	2.3	1.2	5.8	0.0	4.8	1.9	2.0	–	–	–	–	–	−5.56	−20.63
	9610	22.1	7.7	510	3.1	0.4	5.2	0.7	3.1	2.3	2.6	−2.38	0.35	0.83	−2.13	−7.11	−5.65	−29.99
	9505	24.4	7.7	740	1.2	1.0	4.6	0.0	3.0	2.3	2.2	−2.28	0.34	1.02	−2.05	−6.34	−5.9	−31.69
	11795	21.4	7.7	1,200	6.9	5.4	5.9	0.0	12.0	4.0	2.7	−1.67	0.49	0.85	−1.41	−6.14	−5.21	−19.99
	12042	21.3	7.4	950	6.4	2.7	3.8	1.0	5.6	3.4	5.7	−2.14	0.12	0.15	−1.88	−6.04	−5.55	−32.61
	12055	21.1	7.3	670	6.5	1.2	4.6	0.0	6.7	2.2	3.6	−3.11	-0.18	-0.55	−2.85	−6.57	−5.74	−30.93
	12001	21.3	7.4	590	4.0	0.1	3.3	0.0	3.1	1.5	2.8	−2.53	0.04	0.00	−2.27	−6.86	−5.74	−35.75
	13300	24.7	7.2	1,100	2.9	0.5	4.2	0.1	2.2	2.0	3.0	−1.83	0.33	0.25	−1.61	−6.24	−5.65	−33.84
	13400	21.3	7.7	560	6.6	1.2	4.6	0.5	4.5	2.6	6.4	−2.35	0.31	0.62	−2.09	−6.63	−5.86	−32.92
	13000	21.7	7.4	1,070	2.1	1.2	4.9	0.1	5.2	1.5	1.9	−2.69	0.15	0.36	−2.44	−6.70	−5.47	−25.31

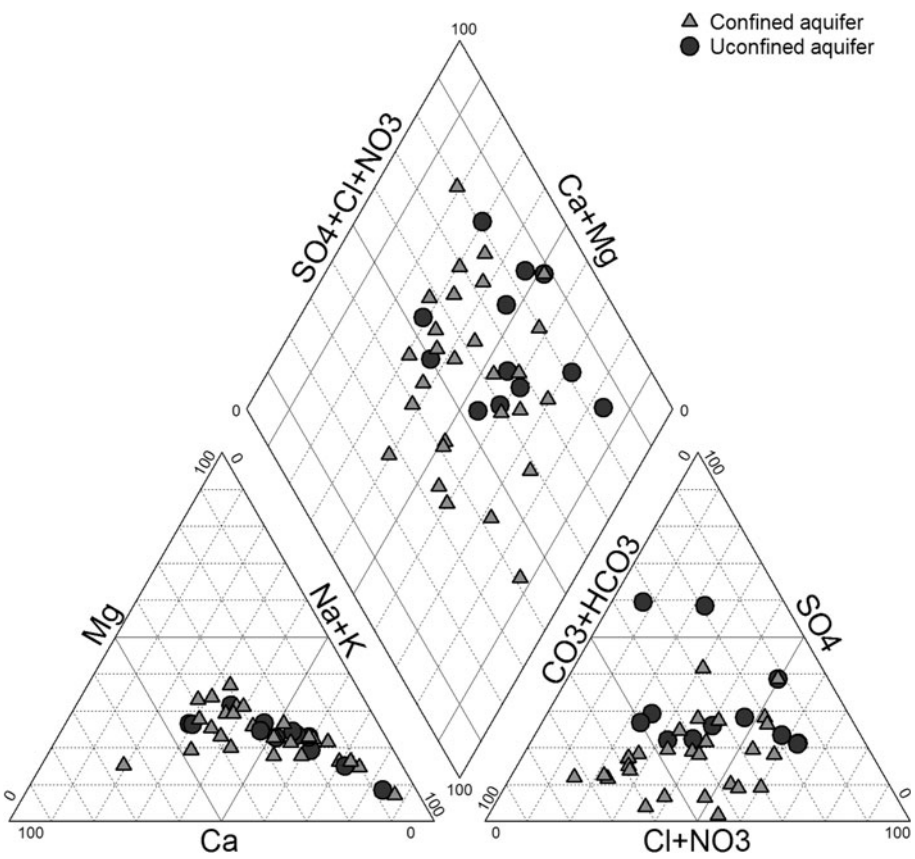

Fig. 4 Piper diagram of the Hammamet–Nabeul deep aquifer system

Isotopic composition of groundwater

Stable isotopes of water molecule are influenced by processes affecting the groundwater rather than the solutes. Thus, they can help to identify groundwaters that have undergone evaporation or mixing with waters from other aquifers (Sacks and Tihansky 1996). Moreover, they can provide reliable information about the mode and origin of groundwater recharge i.e., recharge under different climatic conditions. These processes can be pointed out mainly through the plot of groundwater samples in the $\delta^{18}O/\delta^{2}H$ conventional diagram with respect to the rainfall input function, represented by the Global meteoric water line (GMWL) (Craig 1961) and/or the regional meteoric water line (RMWL).

The $\delta^{18}O$ and $\delta^{2}H$ contents of the Hammamet–Nabeul deep groundwater samples vary from −6.08 to −5.04‰ and from −36.35 to −20‰, respectively. These data were plotted in the $\delta^{18}O/\delta^{2}H$ diagram together with the Weighted mean of regional precipitation (WMRP), the GMWL and the RMWL of the Tunis–Carthage, located at about 60 km from the study area (Fig. 9). Several observations can be made about the stable isotope composition of the Hammamet–Nabeul groundwater samples in relation to each other and to the WMRP. Firstly, most groundwater does not show patterns of enrichment that could be attributed either to evaporation of meteoric water during recharge (Allison 1982) or extensive mineral–water interactions following recharge (Banner et al. 1989). The $\delta^{18}O$ contents reflect, therefore, the conditions present at the time of aquifers recharge. Secondary, all groundwater samples show relatively depleted $\delta^{18}O$ and $\delta^{2}H$ contents with respect to the WMRP. This depletion indicates lower condensation temperature of the precipitation that contributes to the recharge of Hammamet–Nabeul deep aquifer system, which could be attributed either to an altitude effect or to a paleoclimatic effect. Third, most groundwater samples plot between the GMWL and the RMWL, indicating that they are derived from a mixture of oceanic and Mediterranean vapor masses. Fourth, groundwater samples show different clusters according to their position with respect to the RMWL and the WMRP, which suggest different origins of groundwater bodies or intensive exchange with aquifer gasses (Fontes 1976). The first group, constituted mainly by the samples collected from the unconfined level of the aquifer system, is characterized by the more enriched isotopic contents. However, these contents are relatively depleted in both $\delta^{18}O$ and $\delta^{2}H$ relative to the WMRP. This depletion, which is between 0.5 and 0.7 delta for $\delta^{18}O$ and between 5 and 9 delta for $\delta^{2}H$, is presumably

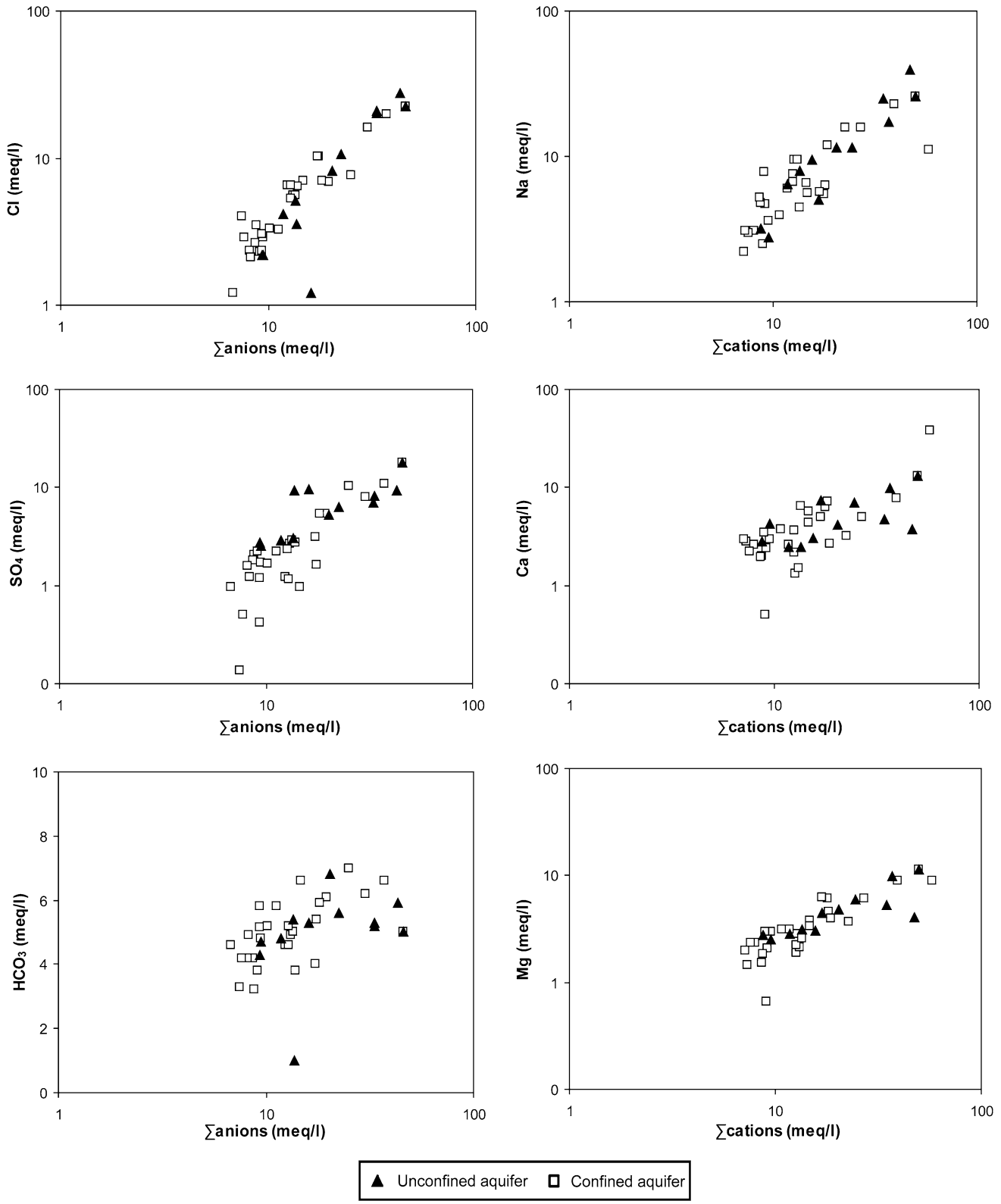

Fig. 5 Plots of Σ anions versus each anion and Σ cations versus each cation

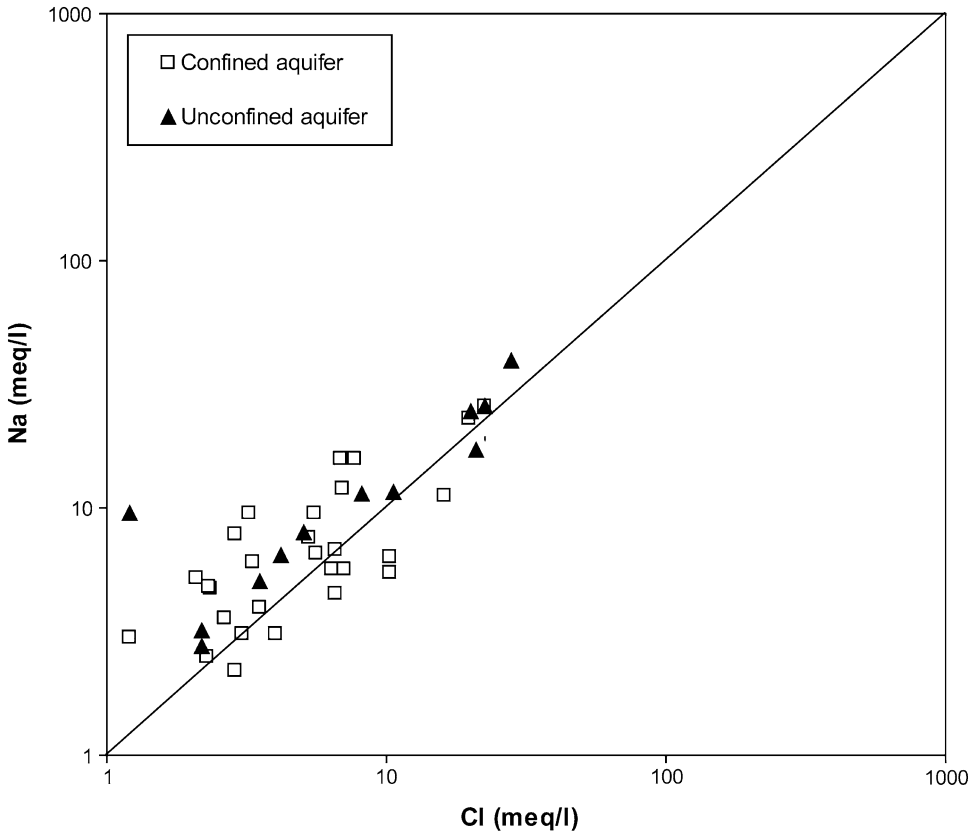

Fig. 6 Plot of Na versus Cl (a)

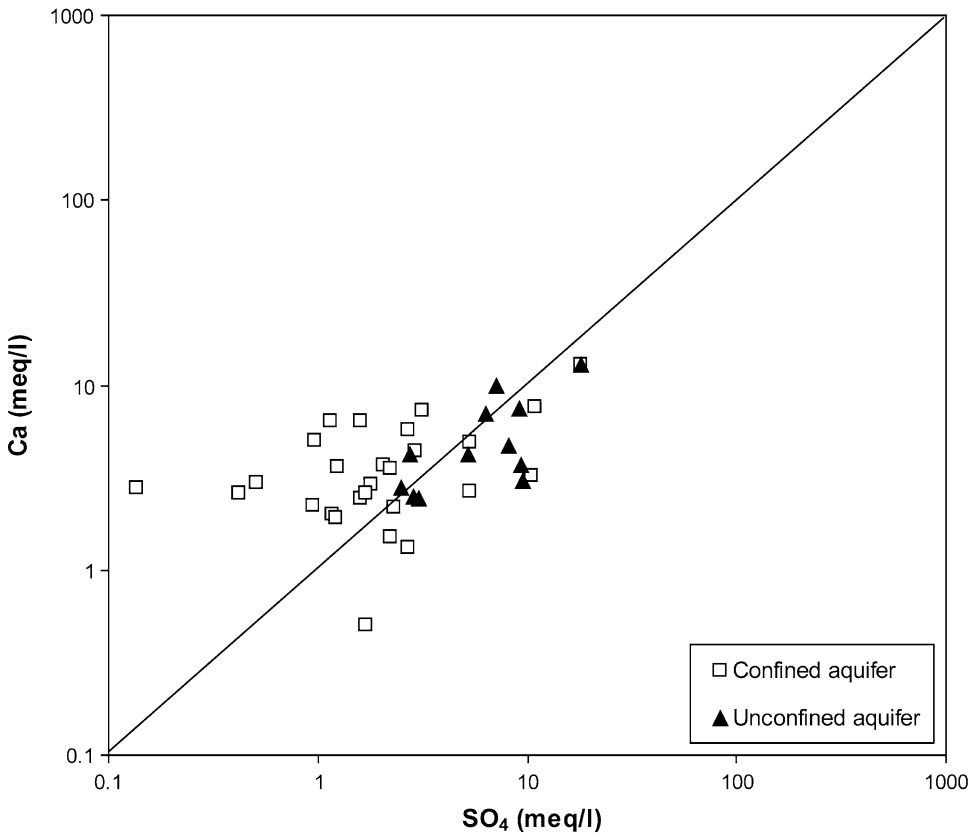

Fig. 7 Plots of Ca versus SO_4

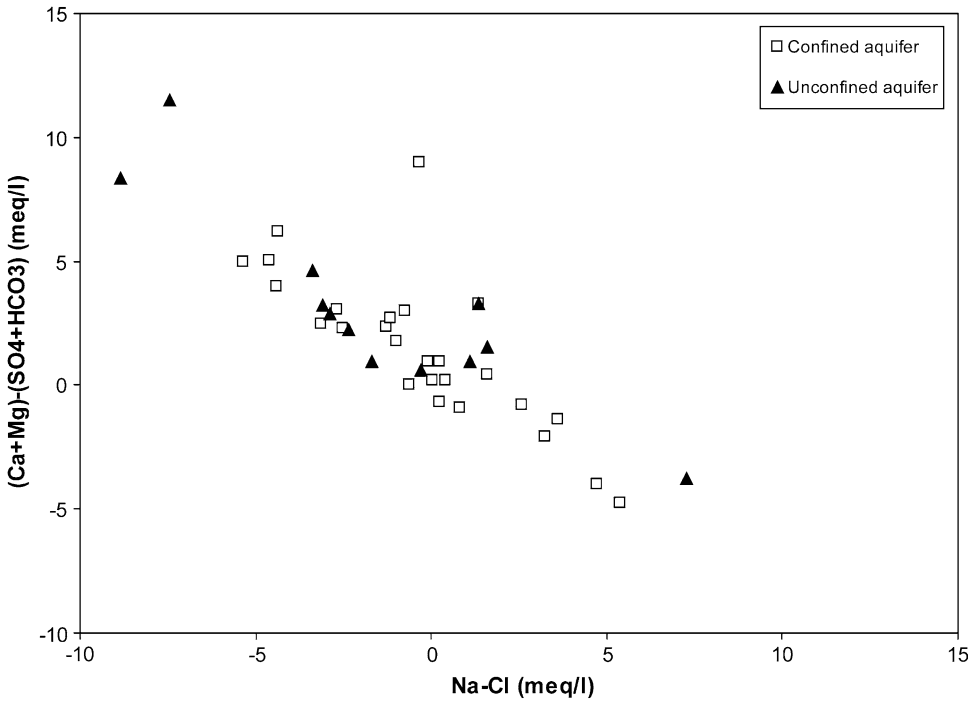

Fig. 8 Plot of $(Na^+ + K^+ - Cl^-)$ versus $[(SO_4^{2-} + HCO_3^-) - (Ca^{2+} + Mg^{2+})]$

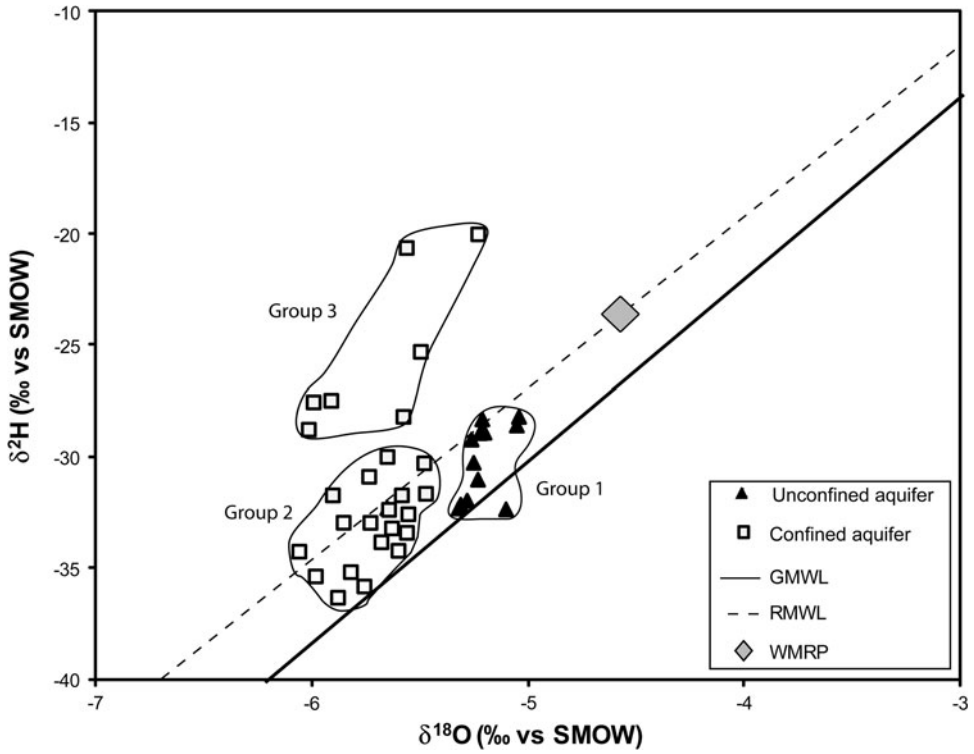

Fig. 9 $\delta^{18}O/\delta^{2}H$ diagram

related to an altitude effect i.e. the aquifer system, has been recharged at altitudes higher than that of the Tunis–Carthage GNIP station for which the WMRP has been calculated. The estimation of the recharge altitudes of the unconfined level can be made by the use of following equation:

$$A_{\text{Recharge}} = A_{\text{GNIP}} + 100(\delta^{18}O_{\text{WMRP}} - \delta^{18}O_{\text{PQ1}}/G) \quad (1)$$

With, A_{Recharge}: estimated altitudes of recharge, A_{GNIP}: altitude of Tunis–Carthage station (4 m amasl), $\delta^{18}O_{\text{WMRP}}$: $\delta^{18}O$ of the WMRP (−4.59), $\delta^{18}O_{\text{PQ1}}$: $\delta^{18}O$ range of variation of the unconfined level (−5.6; −4.6‰), G:

altitudinal gradient of ^{18}O of −0.30‰ per 100 m in precipitation.Considering an ^{18}O altitudinal gradient of −0.30‰ per 100 m in precipitation (Ben Moussa 2011), and taking into account the Eq. 1, the recharge altitude of the referred groundwaters would be between 170 and 240 m. In fact, this range coincides with the altitude of Plio-Quaternary outcrops in the pediments of surrounding mountains, which is between 100 and 340 m.

The second group, which is constituted by the majority of the confined level water samples, is distinguished by the more depleted contents. This depletion is also related either to an altitude effect or to a paleoclimatic effect. However, if it is supposed that these depleted values resulted from an altitude effect, the recharge altitude, estimated according to the Eq. 1 and the ^{18}O altitudinal gradient of −0.30‰ per 100 m, is much higher (between 310 and 510 m) than the aquifer outcrops in the study area, which do not exceed 300 m. This may indicate that the recharge of the confined groundwaters derive from a palaeoclimatic origin.

The third group, which includes a limited number of confined level samples, is also characterized by depleted $\delta^{18}O$ contents comparable to those of the group 2, suggesting also that the recharge of the confined levels has been occurred during a colder climate. However, these samples are unusually displaced to the left of both the GMWL and LMWL, which signify whether the groundwater is ^{2}H-enriched or ^{18}O-deficient (Hamed et al. 2008). Elsewhere, waters lying to the left of the meteoric water line have been regarded as ^{18}O-deficient and this could arise by exchange with the relatively ^{18}O-rich oxygen bound in the surrounding silicate minerals at ambient temperatures (20°–30°C). At these temperatures, the fractionation of ^{18}O between mineral and aqueous phases is relatively large and, given the prolonged residence time of the groundwater, it will become deficient in ^{18}O over geological time (Gascoyne 2004; Hamed et al. 2008). The ^{2}H content would remain essentially unchanged, as the content of ^{2}H in the rocks is very low. However, it is just as possible that the groundwater is ^{2}H-rich and processes of concentrating ^{2}H in the groundwater, such hydrolysis and H_2S-exchange, have been proposed to account for the enrichment. However, it is noteworthy that the boreholes from which were collected the referred groundwater samples are located near the municipal site of domestic waste landfill. This implies that the ^{2}H-enrichement likely results from the exchange with the H_2S in relation with the bacterial reduction of sulfate within the aquifer system.

Summary and conclusion

The hydrochemical investigation indicates that deep groundwaters are mainly influenced by water–rock interaction processes i.e. dissolution of evaporates and cation-exchange process. The sulfate reduction in relation with bacterial activities also plays a significant role in the groundwater salinization for some groundwater samples, especially those located in the vicinity of the municipal site of domestic waste landfill. The stable isotope signatures permit to classify the studied groundwaters into different groups. The first group is characterized by relatively enriched isotope contents indicating the presence of an important component of recent recharge infiltrated at higher altitude. The second group is distinguished by relatively depleted contents of stable isotope reflecting a paleoclimatic origin. The third group is characterized by a significant enrichment of deuterium lending support to an excessive exchange with H_2S related to the bacterial reduction of sulfate. The reliable estimation of groundwater recharge is necessary to improve water management efficiency in order to secure water supply of different socioeconomic sectors. Moreover, groundwater abstraction from the studied aquifer system should be efficiently regarded as development of a non-renewable resource, a fact that is highlighted by the water-table decline in the coastal part of the basin. On the other hand, it would be necessary to utilize a few of tritium and radio-carbon analysis to extend the interpretation of relatively costly research-level investigations. Indeed, the hydrochemical timescale can provide means of evaluating aquifer homogeneity and/or stratification.

References

Allison GB (1982) The relationship between ^{18}O and deuterium in water and in sand columns undergoing evaporation. J Hydrol 76:1–25

Banner JL, Wasserburg GJ, Dobson PF, Carpenter AB, Moore CH (1989) Isotopic and trace-element constraints on the origin and evolution of saline groundwaters from central Missouri. Geochim Cosmochim Acta 53:383–398

Ben Moussa (2011) Etude hydrogéologique, hydrochimique et isotopique de Hammamet–Nabeul, Cap Bon, Tunisie nord-orientale. PhD thesis, University of Sfax, Tunisia. 147

Ben Salem H (1995) Évolution de la péninsule du cap Bon (Tunisie orientale) au cours du Néogène, Notes Service Géologique. Tunisie 61:73–84

Blondel JAT (1991) Les séries à tendance transgressive marine du Miocène inférieur à moyen de la Tunisie centrale [Trangressive series of the Lower and middle Miocene in central Tunisia]. PhD thesis, University of Genova, Italy

Burollet PF (1956) Contribution à l'étude stratigraphique de la Tunisie centrale. Annale des mines et de la géologie, 345

Coleman ML, Shepherd TJ, Durham JJ, Rouse JE, Moore GR (1982) Reduction of water with zinc for hydrogen isotope analysis. Anal Chem 54:993–995

Colleuil B (1976) Etude stratigraphique et néotectonique des formations néogènes et quaternaires de la région de Hammamet–Nabeul (Cap Bon) D.E.S, Université de Nice

Compton JS (1988) Degree of supersaturation and precipitation of organogenic dolomite. Geol. 16:318–321

Craig H (1961) Isotopic variations in meteoric waters. Science 133:1702–1803

DGRE (Direction Générale des Ressources en Eau) (2006) Annuaire de l'exploitation des nappes phréatique de la Tunisie. DGRE, Tunis, Tunisie

Elmejdoub N, Jedoui Y (2009) Pleistocene raised marine deposits of the Cap Bon peninsula (N–E Tunisia): records of sea-level highstands, climatic changes and coastal uplift. Geomorph 112:179–189

Epstein S, Meyada TK (1953) Variations of ^{18}O content of waters from natural sources. Geochimi Cosmochimi Acta 4:213–224

Gascoyne M (2004) Hydrogeochemistry, groundwater ages and sources of salts in a granitic batholith on the Canadian Shield, southeastern Manitoba. Appl Geochem 19:519–560

Gomis-Yagues V, Boluda-Botella N, Ruiz-Bevia F (2000) Gypsum precipitation/dissolution as an explanation of the decrease of sulphate concentration during seawater intrusion. J Hydrol 228:48–55

Hamed Y, Dassi L, Ahmadi R, Ben Dhia H (2008) Geochemical and isotopic study of the multilayer aquifer system in the Moulares-Redayef basin, southern Tunisia. J hydrol Sci 53(C5):1241–1252

Fontes JCh (1976) Isotopes du milieu dans les eaux naturelles. La Houille Blanche 314:205–221

Jorgensen BB (1982) Mineralization of organic matter in the sea bed-the role of sulphate reduction. Nature 296:643–645

Last WM (1990) Lacustrine dolomite an overview of modern, Holocene, and Pleistocene occurrences. Earth Sci Rev 27:221–263

Lyons WB, Long DT, Hines ME, Gaudette HE, Armstrong PB (1984) Calcification of cyanobacterial mats in Solar Lake. Sinai Geol 12:623–626

Mzali H (2010) Etude des déformations et évolution des paléocontraintes dans la région de BouFicha-Grombalia. Thèse de Doctorat en Sciences Géologiques, Univ Tunis El Manar, 164. Classique

Mzali H, Gabtni H, Zouari H, Hadj Sassi M, Gharsalli J (2007) Evidence of N120 shear corridors and associated tectonic structures in north-eastern Tunisia after geological and geophysical data. Comptes Rendus Geoscience 339:358–365

Piper AM (1944) A graphic procedure in the geochemical interpretation of water-analyses. Trans Am Geophys Union 25:914–923

Sacks LA, Tihansky AB (1996) Geochemical and Isotopic Composition of Ground Water, with Emphasis on Sources of Sulfate, in the Upper Floridan Aquifer and Intermediate Aquifer System in southwest Florida. U.S. Geological Survey. Water-Resources Investigations. Technical Report 96–4146

Schoeller H (1939) Le Quaternaire du Golfe ancien de Grombalia, Tunisie, 14–30